Title

Multiparametric MRI identifies and stratifies prostate cancer lesions: Implications for targeting intraprostatic targets

Journal

Brachytherapy, 13(3)

ISSN

1538-4721

Authors

Anderson, Erik S
Margolis, Daniel JA
Mesko, Shane
et al.

Publication Date

2014-05-01

DOI

10.1016/j.brachy.2014.01.011

Peer reviewed

ELSEVIER

Brachytherapy ■ (2014) ■

BRACHYTHERAPY

Multiparametric MRI identifies and stratifies prostate cancer lesions: Implications for targeting intraprostatic targets

Erik S. Anderson[1,2], Daniel J.A. Margolis[3], Shane Mesko[4], Robyn Banerjee[1], Pin-Chieh Wang[1], D. Jeffrey Demanes[1,5], Patrick Kupelian[1], Mitchell Kamrava[1,5,*]

[1]*Department of Radiation Oncology, David Geffen School of Medicine, University of California Los Angeles, Los Angeles, CA*
[2]*Medical Scientist Training Program, University of California Los Angeles, Los Angeles, CA*
[3]*Department of Radiology, University of California Los Angeles, Los Angeles, CA*
[4]*School of Medicine, University of California, Irvine, CA*
[5]*Jonsson Comprehensive Cancer Center, Los Angeles, CA*

ABSTRACT

PURPOSE: To assess the ability of multiparametric (mp) MRI (mp-MRI) to identify, stratify, and localize biopsy-proven prostate cancer lesions in a risk-stratified patient population.

METHODS AND MATERIALS: We retrospectively analyzed 57 patients who had mp-MRI and core needle biopsy during diagnostic prostate cancer evaluation. The MRI sequences were scored for suspicion of cancer with a previously described system. Distributions of mp-MRI scores were compared across National Comprehensive Cancer Network prostate cancer risk groups. The mp-MRI−identified lesions were compared with the location of positive core needle biopsies to assess mp-MRI localization of true lesions.

RESULTS: The mp-MRI scoring system identified lesions in 84% (48/57) of the patients, including 100% (12/12) in the high-risk group. Scores assigned to lesions in patients in intermediate- and high-risk groups were statistically higher than those in the low-risk group, with a relative risk of 6.72 (95% confidence interval: 2.32−19.51, $p < 0.001$) of having an aggressive score assigned in high-risk patients compared with the low-risk patients. In comparing the localization data from core needle biopsy, 68% of the patients had an MRI-identified lesion in or within one adjacent sextant of the same prostate hemigland, including 85% of aggressive lesions.

CONCLUSIONS: Use of mp-MRI at the time of diagnosis can identify intraprostatic lesions and assign suspicion for high-risk disease. These data show that high-risk patients are more likely to have suspicious imaging-identified lesions that correlate to the location of biopsy-proven prostate cancer. At this time, the use of mp-MRI to define focal targets represents a complementary tool to patient evaluation for focal therapy strategies.

Keywords: Multiparametric MRI; Prostate cancer; mp-MRI scoring; Index lesion; MRI-based planning

Introduction

Standard radiation treatment for prostate cancer homogeneously encompasses the whole gland irrespective of the location of positive prostate cancer biopsies. The increasing ability to discern intraprostatic lesions, coupled with recognition that the index lesion is a common site of failure, has led to radiation treatment plans that either dose escalate or only treat the index lesion (1−6). Whether one believes in only treating the index lesion or boosting it, identifying this lesion on MRI with confidence is a critical component of this treatment strategy. The utility of MRI to accurately identify prostate cancer lesions has been demonstrated for many years; however, its sensitivity or specificity is much improved with the incorporation of multiparametric MRI (mp-MRI) (7), for review see Ref. (8). Turkbey *et al.* (9) performed an mp-MRI radiologic histopathologic correlation study using radical prostatectomy specimens and showed a high positive predictive value (PPV) for

Received 6 November 2013; received in revised form 7 January 2014; accepted 28 January 2014.

* Corresponding author. Department of Radiation Oncology, University of California Los Angeles, 200 UCLA Medical Plaza, Suite B265, Los Angeles, CA 90095. Tel.: +1-310-825-9775; fax: +1-310-794-9795.

E-mail address: mkamrava@mednet.ucla.edu (M. Kamrava).

1538-4721/$ - see front matter
http://dx.doi.org/10.1016/j.brachy.2014.01.011

mp-MRI detecting prostate cancer. There was a higher sensitivity for lesions larger than 5 mm in diameter and those with higher Gleason scores.

How best to incorporate this information during the evaluation of patients with prostate cancer is still emerging. Indeed, one recent international consensus statement on focal low-dose-rate brachytherapy for prostate cancer included a recommendation that mp-MRI before biopsy be included whenever possible, and would ideally include anatomic T1/T2 series, functional diffusion, and contrast enhancement series as well as MR spectroscopic data (10). However, as mp-MRI does not detect all foci of prostate cancer and recent data suggest that not all MRI-identified lesions correlate with positive tissue biopsies, how best to integrate these data and the necessity of confirmatory biopsies of mp-MRI–identified lesions are not clear (8, 11). We used a retrospective case study approach to determine whether a lesion scoring system for mp-MRI–defined lesions can stratify them into those that are and are not actually cancer as well as to correlate whether a scoring system can identify higher risk lesions.

Methods and materials

Patient data

Patients with prostate adenocarcinoma who were referred for definitive radiation treatment for biopsy-proven prostate cancer between January 2012 and January 2013 were reviewed. All patients considered had mp-MRI on a 3.0-T Siemens Magnetom Trio (Siemens Medical Solutions, Malvern, PA) including T1-, T2-, diffusion-weighted imaging, and dynamic contrast-enhanced (DCE) pulse sequences. Inclusion required biopsy confirmation of prostate cancer that was performed within 1 calendar year of the mp-MRI evaluation. Risk stratification followed National Comprehensive Cancer Network (NCCN) guidelines for prostate cancer risk assessment (Gleason score, clinical T-stage, and serum prostate-specific antigen). Biopsy data were collected from the review of pathology reports. All patients underwent transrectal nonsaturation biopsies. Six patients underwent ultrasound (US)–MRI fusion–targeted biopsies using the ARTEMIS device, 3 had systematic biopsies using the ARTEMIS device to assist in mapping out and targeting standard systematic biopsy locations, and the remainder (48 patients) underwent standard US-guided systematic biopsies.

Table 1
Multiparametric MRI acquisition specifications

Pulse sequence	TR/TE (ms)	Slice (mm)	Matrix/FOV (cm)	Parameters
T2	4000/101	3.6	320 × 320/17	ETL 25
3D TSE	3800–5040/101	1.5	256 × 256/14	ETL 13
DWI:EPI	3900/60	3.6	130 × 160/21 × 26	b = 0, 100, 400, 800
DCE:TWIST	3.9/1.4 (12° FA)	3.6	160 × 160/26 × 26	See below[a]

TR = repetition time; TE = echo time; FOV = field of view; ETL = echo-train length; TSE = turbo spin echo; EPI = echo planar imaging; TWIST = time-resolved angiography with stochastic trajectories.

Multiparametric MRI sequences were acquired according to the standard methods for functional MRI series.

[a] 4.75 s/Acquisition over 6 min with 15-s injection delay.

MRI analysis

The MRI series were collected per criteria in Table 1, with placement of a pelvic coil in all cases. Image analysis was performed using iCAD VersaVue and OmniLook (Invivo, Gainesville, FL) with Parker arterial input functions for pharmacokinetic analysis. This process uses the Tofts three-compartment model (Ktrans, Kep, and Vp) and also detected initial area under the curve and apparent diffusion coefficient (ADC). Lesions were graded for suspicion using these image series according to the MRI rating scale described previously and reproduced in Table 2 (11). A composite grade was assigned based on a weighted average of scores assigned for lesion appearance by T2 and DCE series, as well as by calculated ADC as has been previously described (11, 12). Using this grading system, lesions were scored from one to five in which a score of one indicates no suspicion for cancer, whereas scores two through five indicate increasing suspicion of prostate cancer.

Data analysis

After assignment of image grades to the MRI-defined lesions, the targets were separated into categories of "low

Table 2
Multiparametric MRI classification system

Image grade	T2-weighted imaging	Apparent diffusion coefficient ($\times 10^{-3}$ m^2/s)	Dynamic contrast enhancement
1	Normal	>1.4	Normal
2	Faintly decreased signal	1.2–1.4	Early or intense enhancement
3	Distinct low signal	1.0–1.2	Early and intense enhancement, or early enhancement with washout
4	Markedly decreased signal	0.8–1.0	Early and intense enhancement with washout
5	Focal low signal with mass effect	<0.8	Early enhancement is intense with immediate washout

DWI = diffusion-weighted imaging; DCE = dynamic contrast enhancement.

Lesions identified on multiparametric MRI series were assigned a susceptibility score that integrated components from T2, DWI, and DCE functional series, as reported previously (8).Reproduced from Sonn *et al.* (11).

suspicion'' (MRI score: 1−3) or ''high suspicion'' (MRI score: 4−5). For localization analysis, the MRI lesions were separated into hemiglands and categorized as a match (MRI and biopsy agree on both hemiglands), a miss (MRI and biopsy disagree on both hemiglands), or a partial match (in which one hemigland is a match and the other is not). Using the total number of hemiglands, specificity, sensitivity, and PPV and negative predictive value (NPV) were calculated. Finally, for each of the cases, the location of positive core biopsies were compared with the location of MRI-identified lesions to determine how often a positive biopsy was found in the same or an adjacent prostate sextant as an MRI-identified lesion. Permitting matches in adjacent sextants in the same hemigland accounts for the variability of biopsy site as well as the fact that MRI typically describes only the center of the tumor, as opposed to its full extent.

Statistical analysis

Statistical analysis of mp-MRI score correlation to risk group and positive core biopsy location was done using a Poisson regression model to examine each factor's association with the score. The relative risk (RR) ratio of the increasing scores was calculated from the regression models with 95% confidence intervals (CIs). Significant difference from the null hypothesis was set at a p-value lower than 0.05 indicating a 95% CI for the ratio that excludes the value of one. Statistical performance calculations for hemigland localization analysis were performed with the following calculations: MRI specificity = (MRI true negative reads/total negative biopsies), MRI sensitivity = (MRI true positive reads/total positive biopsies), MRI PPV = (MRI true positive reads/total MRI positive reads), and MRI NPV = (MRI true negative reads/total MRI negative reads).

Results

A total of 68 patients were identified who were referred for definitive treatment between January 2012 and January 2013 and had mp-MRI imaging during their initial work up. To standardize the data set, patients were excluded for having mp-MRI scans on a 1.5-T scanner ($n = 6$) and for having more than 365 days between MRI and biopsy ($n = 5$), leaving a total of 57 patients. Patient characteristics are summarized in Table 3. The distribution of patients by NCCN risk group was: low: 22, intermediate: 23, and high: 12. At the time of biopsy, 9 of the 57 patients underwent the procedure with a fused MRI and US device to enhance visualization of the prostate. Furthermore, 6 of those patients had specific prostate lesions targeted for biopsy using the ARTEMIS MRI−US fusion device, as their biopsies were performed during the time period of adoption of MRI−US fusion at this institution. All 6 of these patients were of intermediate or high risk, and each had MRI susceptibility scores of four or five. To investigate the impact of these targeted biopsies on these results, we also analyzed the cohort of patients who underwent nontargeted biopsies alone.

Table 3
Patient characteristics ($n = 57$)

Characteristics	n (% or Range)
NCCN Risk Group	
Low	22 (39)
Intermediate	23 (40)
High	12 (23)
Mean age, range	64 (41−83)
Mean PSA, range	8.6 (0.6−90)
Clinical T-stage	
T1c	36 (63)
T2	17 (30)
T3	4 (7)
Biopsy type	
Non-MRI guided, systematic	48 (84)
MRI guided, systematic	3 (5)
MRI guided, targeted	6 (11)
Gleason score	
6	23 (40)
7	24 (42)
8−9	10 (18)
Mean number of core biopsies, range	12.6 (6−21)
Mean positive core biopsy, % (range)	37 (6−100)
3-T MRI	57 (100)
Mean days between multiparametric MRI and biopsy, range	100 (6−360)

NCCN = National Comprehensive Cancer Network; PSA = prostate-specific antigen.

A total of 57 patients met inclusion criteria and were retrospectively analyzed for mp-MRI−identified lesions and the correlation of their score with risk group as well as positive core needle biopsy location.

The mp-MRI detected lesions in 48 of 57 (84%) cases of the patients with biopsy-proven prostate cancer. The ability of mp-MRI to detect any lesion increased as the NCCN risk group increased. Figure 1a shows that mp-MRI lesion detection was 15 of 22 (68%) in low-, 21 of 23 (91%) in intermediate-, and 12 of 12 (100%) in high-risk patients. Using the Poisson regression model, we found significantly increased mp-MRI susceptibility scores in the high- and intermediate-risk groups when compared with the low-risk group. In the high-risk group, the RR of having a higher MRI score was 1.98 (95% CI: 1.35−2.91; $p < 0.001$), and similarly the RR in the intermediate-risk group was 1.51 (95% CI: 1.06−2.15; $p = 0.02$). These findings were statistically significant after exclusion of the patients who underwent targeted biopsy. When compared with low-risk, the RR of a higher mp-MRI score was 1.96 in high-risk (95% CI: 1.29−2.96; $p = 0.002$) and 1.45 in the intermediate-risk group (95% CI: 1.01−2.10; $p = 0.05$).

We next investigated whether patients in higher NCCN risk groups were more likely to be assigned a higher prostate cancer suspicion score. To assess this hypothesis, a suspicion score of one to three was categorized as ''low suspicion'' and scores four to five were categorized as ''high suspicion.'' In total, mp-MRI classified 47.4% (27/57) of tumors as high suspicion (Fig. 1b). By NCCN risk

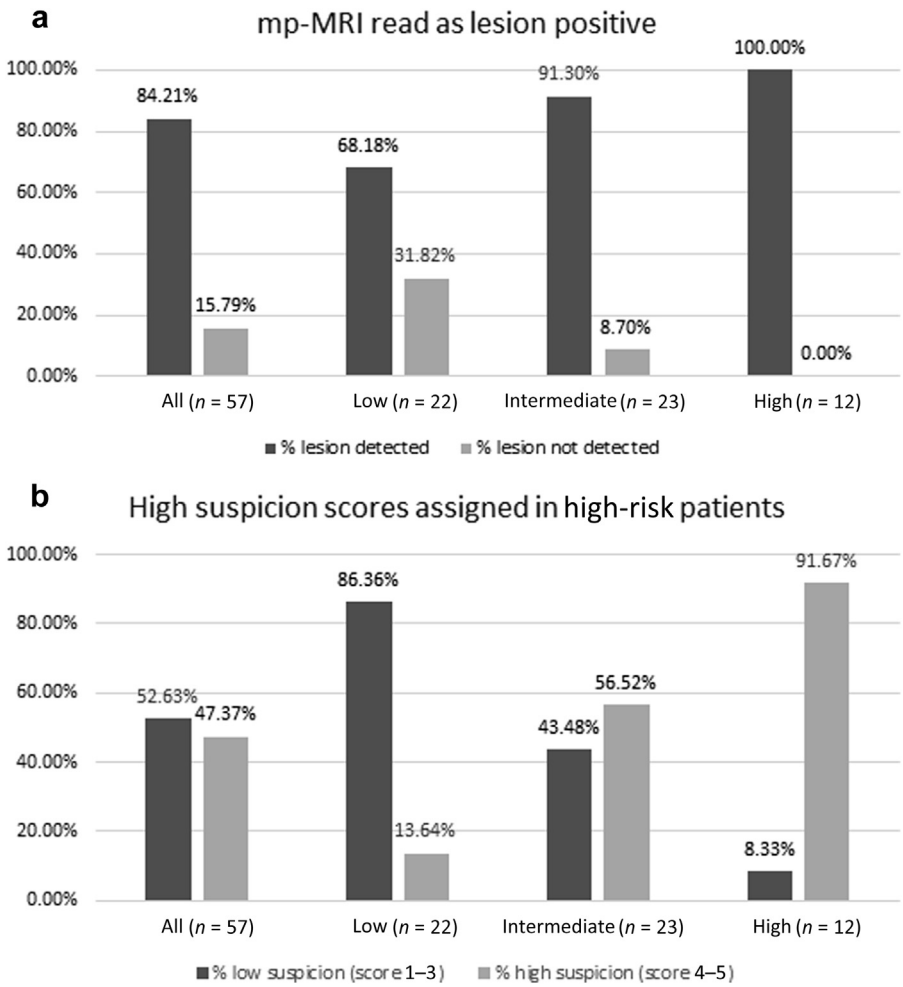

Fig. 1. The mp-MRI detects and differentiates high-risk prostate cancers. (a) Detection of prostate cancers of all MRI grades (1 = no tumor detected, 2−5 = tumor detected), separated by National Comprehensive Cancer Network (NCCN) risk category. (b) Shown are the percentage of detected tumors that are graded as high suspicion (grade: 4−5) vs. low suspicion (grade: 1−3) in all cases as well as separated by the NCCN risk group. Increase in mp-MRI grade in high-risk group was significantly different when compared with both low and intermediate groups (low vs. high, $p < 0.001$; intermediate vs. high, $p = 0.005$). mp-MRI = multiparametric MRI.

group, 11 of 12 (91.7%) lesions in the high-risk group were scored as high suspicion, whereas only 13 of 23 (56.5%) in the intermediate- and 3 of 22 (13.6%) in the low-risk groups were called highly suspicious. We compared high-suspicion mp-MRI scores (scores: 4−5) in the low-risk group independently to both the high- and intermediate-risk groups and found them to be statistically significant by Poisson regression analysis—high vs. low: RR: 6.72 (95% CI: 2.32−19.51; $p < 0.001$) and intermediate vs. low: RR: 4.14 (95% CI: 1.36−1.59; $p = 0.012$). Again, the findings were similar after exclusion of the patients who underwent targeted biopsy. In patients with systematic biopsies, the RR of having a high-suspicious mp-MRI score was 6.52 for the high-risk patients (95% CI: 2.22−19.13; $p < 0.001$) and 3.67 in the intermediate-risk patients (95% CI: 1.17−11.46; $p = 0.03$).

To assess whether mp-MRI−identified lesions were actually cancer, we compared the location of MRI-identified lesions with the location of positive biopsies. For all 57 cases, the prostate was divided into a hemigland with the urethra defining the midline. Hemiglands were used for locational analysis as mp-MRI reports noted the prostatic region that contained the center of the tumor focus, and not the full extent of the lesion. We categorized each case into a match (MRI lesion location and positive biopsy in the same hemigland), a miss (MRI lesion location and positive biopsy location are discordant), or partial match (MRI lesion location and positive biopsy are concordant in one hemigland but not the other) with results given in Table 4. Matches were found in 28 of 57 (49%) cases; however, when a lesion was scored as four to five, 18 of 27 (67%) of cases were a match ($p = 0.018$). A total of 22 of 57 (44%) cases were classified in the match/miss category.

Given the relatively high number of match/miss cases, we evaluated the sensitivity, specificity, NPV, and PPV of mp-MRI−defined lesions being concordant with systematic biopsy results on a hemigland basis. As shown in Table 4,

Table 4
Performance of multiparametric MRI in localizing prostate cancer lesions

MRI rating	All	1−3	4−5
Whole glands (total)	57	30	27
Match (%)	28 (49)	10 (33)	18 (67)
Miss (%)	4 (7)	3 (10)	1 (4)
Partial match (%)	25 (44)	17 (57)	8 (30)
Sextant correlation between MRI and core biopsy (%)	38 (67)	15 (50)	23 (85)
Hemiglands (total)	114	60	54
Positive: true (total)	54 (63)	21 (27)	33 (36)
Negative: true (total)	25 (51)	14 (33)	11 (18)
MRI specificity	0.675	0.525	0.825
MRI sensitivity	0.735	0.700	0.786
MRI positive predictive value	0.857	0.778	0.917
MRI negative predictive value	0.490	0.424	0.611

Positive core biopsies and imaging-defined lesions were compared on a whole gland and hemigland level to determine correlation of positive findings.

the overall specificity of mp-MRI was 0.675 and increased to 0.825 when only considering lesions with MRI ratings of four to five. Additionally, the PPV of mp-MRI−identified lesions was 0.857 for all cases and 0.917 for lesions with MRI scores of four to five.

Given that an MRI score of four to five correlated with positive biopsy location in two-thirds of cases at the hemigland level, we next sought to refine this accuracy by determining whether mp-MRI−identified lesions correlate with positive biopsy locations on a sextant level. For this analysis, each prostate gland was divided into equal sextants: apex, mid, and base regions on both the right and left side of the gland (urethra served as midline). A positive match meant that the MRI-identified lesion corresponded to the same or adjacent sextant in the same hemigland that also contained a positive core biopsy. For example, in the hemigland analysis described previously, a positive right side match above could be negative in this analysis if the MRI lesion was in the right apex of the prostate, whereas positive biopsies were only yielded from the right base of the prostate gland, but would be positive if positive biopsies were yielded from either the right apex or midgland. Allowing matches on the same side of the urethra in adjacent sextants accounts for the variability of biopsy site and the fact that MRI location typically describes the center of the tumor, as opposed to its full extent. All lesions correlated with a positive core biopsy in 66.7% of the cases (38/57; Table 4), and positive matches were statistically more likely to have higher MRI suspicion scores (RR: 1.53, 95% CI: 1.10−2.15, $p = 0.01$). For lesions with an MRI score of one to three, a total of 15 of the 30 cases (50.0%) were a match. In contrast, for lesions with an MRI score of four to five, a total of 23 of the 27 cases (85.1%) were a match, and in these high-suspicion lesions, biopsy matches were statistically more likely to be a match than compared with low suspicion lesions by MRI (MRI score: 4−5 vs. 1−3, RR: 2.88, 95% CI: 1.16−7.13, $p = 0.02$). We repeated the localization analysis after exclusion of the patients who underwent targeted biopsy and found that the RR of having a higher mp-MRI score was 1.46 (95% CI: 1.04−2.07; $p = 0.03$), and there remained a greater likelihood to find a positive match in patients with high suspicion scores as compared with low suspicion scores (MRI score: 4−5 vs. 1−3, RR: 2.52, 95% CI: 1.00−6.39, $p = 0.05$).

Discussion

Treating the whole gland is the current standard of care for prostate cancer radiotherapy. Whether this is actually necessary or whether men would do just as well by either only treating the index lesion is not known. Currently, multiple clinical trials are investigating focused treatment of index lesions; however, at this point in time, there is no consensus on how best to identify and target such lesions (13, 14). One approach entails saturation biopsies to map out the full extent of the disease (15), whereas another is to use mp-MRI to characterize the extent of significant prostate cancer (16, 17). Herein, we investigated whether a scoring system could help characterize whether an mp-MRI−identified lesion is cancer and whether it differentiates lesions that are known to be of different risk categories. The clinical utility of a scoring system would be to stratify patients into groups who have a very high likelihood of an aggressive cancer, which might benefit from a targeted approach, and therefore justify targeted biopsy confirmation, vs. those who are less likely to harbor significant disease. Additionally, a suspicion score for a lesion seen on mp-MRI can provide additional stratification data that could be incorporated into treatment planning strategies such as pursuing active surveillance vs. proceeding with definitive treatment.

We found that mp-MRI at the time of prostate cancer diagnosis detects an increasing number of lesions going from low- to high-risk prostate cancer. This is consistent with data suggesting that the sensitivity of mp-MRI is best for larger and higher Gleason grade lesions (2). Analysis of mp-MRI−identified lesions using a one to five scoring system also revealed that lesions in high-risk patients had consistently higher MRI scores compared with low- or intermediate-risk patients. Given that the MRI scoring system heavily weights the ADC score, this is also consistent with data demonstrating a correlation between Gleason score and ADC values (18).

Our data also show that mp-MRI−identified lesions correlate with tumor location within the prostate as confirmed by systematic prostate cancer biopsies. There is greater agreement at the hemigland than sextant level and among lesions with higher MRI scores (4−5). These results echo the findings of improved accuracy of mp-MRI for higher grade disease and emphasize that, even for high-risk patients, strategies based solely on mp-MRI should be done with caution. Additional studies investigating MRI imaging and pathology correlation are needed to improve our understanding of the ideal radiation treatment volume (CTV and PTV) margins for MRI-based targets.

Previous studies have assessed the ability of mp-MRI to detect and score prostate cancer lesions of biopsy-proven pathologic grade. In a recent study by Sonn *et al.* (11), the reported concordance rate between mp-MRI lesions scored four to five and positive biopsy was nearly 90%, whereas in this present study, we find a concordance rate of 85% in lesions with scores of four to five. The similarities in this finding are significant, given that most patients in this study underwent systematic (nontargeted) biopsies, whereas the previous reports were targeted biopsies (11). The results presented here are underscored by the similarities with or without inclusion of the patients who underwent targeted biopsy, as lesions with high suspicion scores were strongly correlated to positive biopsies in high-risk patients regardless of the biopsy method. The strength of this study and other analyses comparing MRI with biopsies is imparted by the fact that image-identified lesions are compared with pathologic specimens to validate the method. Studies using only imaging methods to track response rates are hindered by the fact that the true nature of a lesion was not known, which could lead to imprecise results given the suggestion from our data and others that MRI and pathology results are not entirely concordant.

This study has a few noteworthy limitations, with the first being a retrospective correlation of lesions identified on MRI with systematic biopsies. The nature of this analysis creates an inhomogeneous patient group that is most appropriately analyzed on a per-patient basis and makes comparison across patients or across studies difficult. A properly controlled prospective study would allow a more homogenous patient population for analysis. There is also the difficulty that, for these MRI reports, only the center location of the lesion is described, and whether it encompassed additional sextant locations was not explicit. Additionally, the MRI score was obtained directly from patient's radiology reports and a radiologist was not asked to go back to reevaluate these lesions for this study. Whether the MRI scores would be changed if one radiologist read the scans is not clear. Most biopsies in this study were nontargeted and none were saturation biopsies, which increases the possibility that tissue sampling in each case was not sufficient to detect all cancer. Undersampling of transrectal ultrasound−guided biopsies is well known and is a potential source of error in this study (19). This could lead to an apparently false-negative lesion on mp-MRI when compared with biopsy results, although even with this potential source of error, a high rate of concordance between imaging and pathologic results was found in this study. A gold standard analysis to evaluate the MRI scoring system described here would be comparison to radical prostatectomy samples, which has previously shown that mp-MRI does reliably identify prostate tumors (20).

For the localization analysis, the division of the prostate into hemiglands and sextants for finer analysis is not as precise as previously described divisions of the prostate into 16 or even 27 regions. This study did show significant correlation between the center of an MRI-identified lesion, as well as reported sextant of biopsy; however, future analyses would benefit from finer localization. This would necessitate knowing the exact biopsy location as well as a more comprehensive description of the extent of the lesion on MRI. Having these additional data would strengthen these analyses; however, the exact biopsy locations were not available for analysis as these were not recorded during the standard transrectal ultrasound−guided biopsies.

With these limitations considered, the fact that the data are consistent with previously published data using the same scoring system demonstrates a robustness and reproducibility of the scoring system (11). Of note, calculation of ADC and pharmacokinetic parameters remains somewhat unstandardized, and a consensus method for their determination has not yet been established. Another limitation is the retrospective gathering of data that was controlled for a maximum of 12 months between MRI and biopsy but neither performed with a consistent temporal relationship nor other patient factors. The variation in time between MRI and biopsy is a potential source of bias within the results presented here, and underscores the fact that close timing of the MRI immediately before biopsy will likely yield the most informative relationship between imaging and pathologic findings. Finally, the mp-MRI series that were used in this analysis included T2-, diffusion-weighted imaging, and DCE, which yielded significant associations with prostate cancer risk status. Additional functional data, including spectroscopy, is likely to augment the performance of mp-MRI during prostate cancer evaluation but is not routinely performed at our institution (10). Continued prospective studies with more enrolled patients who are able to control for these parameters will be necessary to further refine these findings.

The data presented here represents a novel analysis of the utility of mp-MRI imaging during the initial diagnostic work up for prostate cancer. The ability to detect and localize suspicious lesions has implications for less invasive staging as well as to guide focal radiation therapy planning, as has recently been recommended by a consensus statement concerning focal low-dose-rate treatment of prostate cancer (10). It emphasizes the point that a scoring system derived from imaging-identified parameters can be used to define the suspicion of lesions for cancer and their aggressiveness. The mp-MRI scoring presented here has provided consistent results, and a widely accepted scoring system using the similar parameters, such as the recently proposed prostate imaging reporting and data system method (PI-RADS), will likely of benefit to standardize mp-MRI evaluation and incorporation into clinical practice (21). The value of mp-MRI at this time appears to be greatest for identifying and characterizing higher grade disease.

Conclusions

The use of mp-MRI at the time of diagnosis can identify intraprostatic lesions and assign suspicion for high-risk disease. Confirmation of MRI target lesions is necessary as not

all MRI targets are actually cancer, but these data show that patients with high-risk prostate cancer are more likely to have imaging-identified lesions that are assigned higher scores reflecting aggression. At this time, the use of mp-MRI to define focal targets represents a complementary tool to patient evaluation for focal therapy strategies.

References

[1] Bauman G, Haider M, Van der Heide UA, *et al*. Boosting imaging defined dominant prostatic tumors: A systematic review. *Radiother Oncol* 2013;107:274−289.

[2] Turkbey B, Choyke PL. Multiparametric MRI and prostate cancer diagnosis and risk stratification. *Curr Opin Urol* 2012;22:310−315.

[3] Cosset JM, Cathelineau X, Wakil G, *et al*. Focal brachytherapy for selected low-risk prostate cancers: A pilot study. *Brachytherapy* 2013;12:331−337.

[4] Cellini N, Morganti AG, Mattiucci GC, *et al*. Analysis of intraprostatic failures in patients treated with hormonal therapy and radiotherapy: Implications for conformal therapy planning. *Int J Radiat Oncol Biol Phys* 2002;53:595−599.

[5] Pucar D, Hricak H, Shukla-Dave A, *et al*. Clinically significant prostate cancer local recurrence after radiation therapy occurs at the site of primary tumor: Magnetic resonance imaging and step-section pathology evidence. *Int J Radiat Oncol Biol Phys* 2007;69:62−69.

[6] Arrayeh E, Westphalen AC, Kurhanewicz J, *et al*. Does local recurrence of prostate cancer after radiation therapy occur at the site of primary tumor? Results of a longitudinal MRI and MRSI study. *Int J Radiat Oncol Biol Phys* 2012;82:e787−e793.

[7] Wefer AE, Hricak H, Vigneron DB, *et al*. Sextant localization of prostate cancer: Comparison of sextant biopsy, magnetic resonance imaging and magnetic resonance spectroscopic imaging with step section histology. *J Urol* 2000;164:400−404.

[8] Muller BG, Futterer JJ, Gupta RT, *et al*. The role of magnetic resonance imaging (MRI) in focal therapy for prostate cancer: Recommendations from a consensus panel. *BJU Int* 2014;113:218−227.

[9] Turkbey B, Mani H, Shah V, *et al*. Multiparametric 3T prostate magnetic resonance imaging to detect cancer: Histopathological correlation using prostatectomy specimens processed in customized magnetic resonance imaging based molds. *J Urol* 2011;186:1818−1824.

[10] Langley S, Ahmed HU, Al-Qiasieh B, *et al*. Report of a consensus meeting on focal low dose rate brachytherapy for prostate cancer. *BJU Int* 2012;109(Suppl. 1):7−16.

[11] Sonn GA, Natarajan S, Margolis DJ, *et al*. Targeted biopsy in the detection of prostate cancer using an office based magnetic resonance ultrasound fusion device. *J Urol* 2013;189:86−91.

[12] Natarajan S, Marks LS, Margolis DJ, *et al*. Clinical application of a 3D ultrasound-guided prostate biopsy system. *Urol Oncol* 2011;29:334−342.

[13] Memorial Sloan-Kettering Cancer Center. Assessing the potential for reduced toxicity using focal brachytherapy in early stage, low volume prostate Cancer. ClinicalTrials.gov Available at: http://clinicaltrials.gov/ct2/show/NCT01354951. Initiated May 2011. Accessed February 2014. NLM Identifier: NCT01354951.

[14] Lips IM, van der Heide UA, Haustermans K, *et al*. Single blind randomized phase III trial to investigate the benefit of a focal lesion ablative microboost in prostate cancer (FLAME-trial): Study protocol for a randomized controlled trial. *Trials* 2011;12:255.

[15] Ahmed HU, Akin O, Coleman JA, *et al*. Transatlantic Consensus Group on active surveillance and focal therapy for prostate cancer. *BJU Int* 2012;109:1636−1647.

[16] Arumainayagam N, Ahmed HU, Moore CM, *et al*. Multiparametric MR imaging for detection of Clinically significant prostate Cancer: A validation cohort study with transperineal template prostate mapping as the reference standard. *Radiology* 2013;268:761−769.

[17] Yerram NK, Volkin D, Turkbey B, *et al*. Low suspicion lesions on multiparametric magnetic resonance imaging predict for the absence of high-risk prostate cancer. *BJU Int* 2012;110:E783−E788.

[18] Nagarajan R, Margolis D, Raman S, *et al*. MR spectroscopic imaging and diffusion-weighted imaging of prostate cancer with Gleason scores. *J Magn Reson Imaging* 2012;36:697−703.

[19] Han M, Chang D, Kim C, *et al*. Geometric evaluation of systematic transrectal ultrasound guided prostate biopsy. *J Urol* 2012;188:2404−2409.

[20] Villers A, Puech P, Mouton D, *et al*. Dynamic contrast enhanced, pelvic phased array magnetic resonance imaging of localized prostate cancer for predicting tumor volume: Correlation with radical prostatectomy findings. *J Urol* 2006;176:2432−2437.

[21] Barentsz JO, Richenberg J, Clements R, *et al*. ESUR prostate MR guidelines 2012. *Eur Radiol* 2012;22:746−757.